Supporting Information

Drost et al. 10.1073/pnas.1220537110

SI Materials and Methods

Crystal Structure Modeling. Crystal structures were visualized using PyMOL software (Delano Scientific), using the Protein Database file from the published human MutS Homolog 2/6 crystal structure (Molecular Modeling Database ID #53938) (1).

Determination of Genomic Mutator Phenotypes at the Hypoxanthine Phosphorybosyl Transferase (*Hprt*) Gene. Spontaneous mutagenesis at the monoallelic genomic *Hprt* gene was determined essentially as described (2). Briefly, cell lines were cultured in hypoxanthine-aminopterin-thymidine (HAT)-supplemented medium for two subsequent passages to eliminate any preexisting *Hprt*-deficient cells, after which cell lines were propagated for three passages in the absence of HAT to allow the accumulation of spontaneous mutations at *Hprt*. Cells were then continuously cultured in medium containing 60 μM 6-thioguanine (Sigma-Aldrich) to select for *Hprt*-deficient clones. Of note, mismatch repair (MMR)-deficient (but *Hprt*-proficient) cells do not survive these stringent selection conditions. After 10 d, *Hprt*-deficient colonies were fixed, stained, and counted. Counts were corrected for cloning efficiencies.

Microsatellite instability was analyzed by isolating ∼50 subclones of each *Msh2*-mutant cell line. From these subclones, genomic DNA was isolated by Proteinase K lysis, and microsatellite sizes were determined after amplification by PCR and subsequent fragment analysis, as described previously (3). Data were analyzed using GeneMarker software (Softgenetics).

Methylation Tolerance Assays. *Msh2*-mutant cells were treated with *N*-Methyl-*N*′-Nitro-*N*-Nitrosoguanidine and, simultaneously, O^6-benzylguanine, an inhibitor of the repair enzyme methyl guanine methyl transferase, as described (4). After 3 d, adhering cells were counted, survival relative to the untreated cells was calculated, and the IC_{50} was determined.

In Vitro MMR Assays. MMR assays to test humanized variant MMR proteins were performed as described (5). To test MMR activity in cell extracts from the validation panel, 130 μg cytoplasmic extract was assayed in the absence or presence of 100 ng recombinant wild-type human MSH2/MSH6. (kindly provided by T. Sixma, The Netherlands Cancer Institute, Amsterdam, the Netherlands). The results for these experiments were verified in a second set of experiments, using independent batches of cell extracts.

Western Blotting. Analysis of Msh2 and Msh6 protein expression by Western blotting was performed as described (4).

Electrophoretic Mobility Shift Assays. Oligonucleotide sequences were as described (6). One hundred seventy femtomole double-stranded matched or mismatched (G·T) oligonucleotide, labeled at the 5′ end using γ-^{32}P ATP and polynucleotide kinase, was incubated with 20 μg cytoplasmic extract in 1× DNA binding buffer [12% (vol/vol) glycerol, 20 mM Hepes/KOH at pH 7.9, 100 mM NaCl, 1 mM DTT, and 0.1 mM EDTA, with 0.05 μg/μL Poly(deoxynosinic-deoxycytidylic) acid sodium salt and 425 fmol unlabeled, matched oligonucleotide] for 20 min at 37°C in a total volume of 20 μL. For adenine nucleotide challenge experiments, ATP was added 10 min after addition of the DNA probe. The reaction mixture was subjected to electrophoresis in a 4% polyacrylamide:bisacrylamide (29:1) gel in 0.5× TBE buffer containing 5% glycerol. The gels were dried, signals were visualized using a Cyclone Plus Phosphor Imager (PerkinElmer), and images were analyzed using OptiQuant software.

1. Warren JJ, et al. (2007) Structure of the human MutSalpha DNA lesion recognition complex. *Mol Cell* 26(4):579–592.
2. Borgdorff V, Pauw B, van Hees-Stuivenberg S, de Wind N (2006) DNA mismatch repair mediates protection from mutagenesis induced by short-wave ultraviolet light. *DNA Repair (Amst)* 5(11):1364–1372.
3. Bacher JW, Abdel Megid WM, Kent-First MG, Halberg RB (2005) Use of mononucleotide repeat markers for detection of microsatellite instability in mouse tumors. *Mol Carcinog* 44(4):285–292.
4. de Wind N, et al. (1999) HNPCC-like cancer predisposition in mice through simultaneous loss of Msh3 and Msh6 mismatch-repair protein functions. *Nat Genet* 23(3):359–362.
5. Drost M, et al. (2012) A rapid and cell-free assay to test the activity of lynch syndrome-associated MSH2 and MSH6 missense variants. *Hum Mutat* 33(3):488–494.
6. Lützen A, de Wind N, Georgijevic D, Nielsen FC, Rasmussen LJ (2008) Functional analysis of HNPCC-related missense mutations in MSH2. *Mutat Res* 645(1-2):44–55.

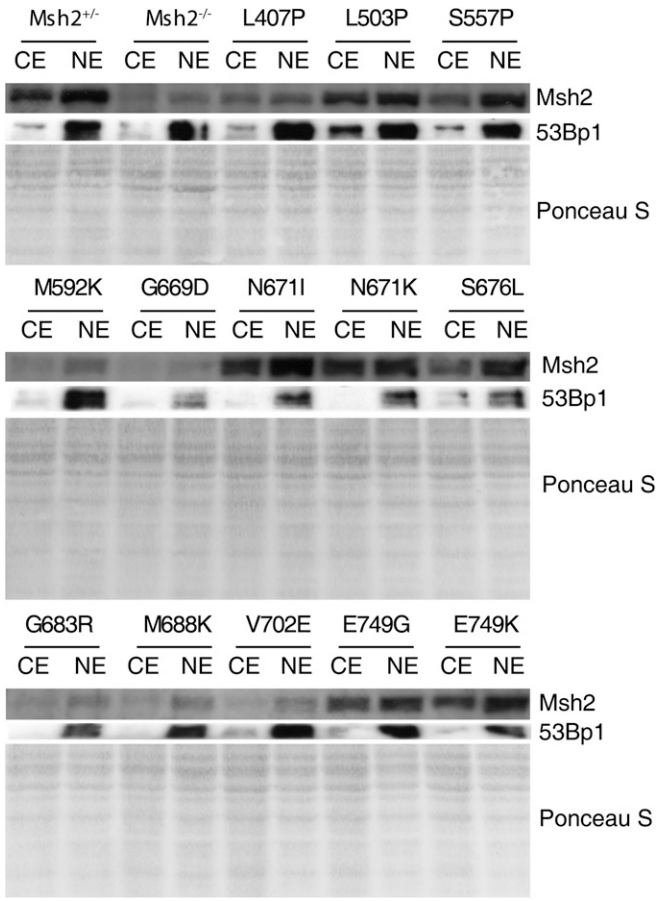

Fig. S1. Western blot analysis of cytoplasmic and soluble nuclear extracts (CE and NE, respectively) of mutant cell lines. p53-binding protein 1 (53Bp1) is used as a nuclear marker. Ponceau S staining reveals equal loading of extracts.

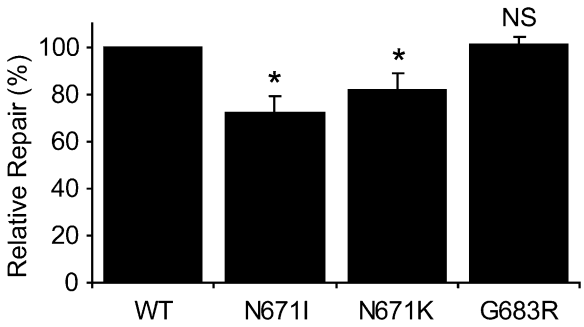

Fig. S2. Inhibition of in vitro mismatch repair in HeLa cell extracts by in vitro expressed variants. MMR substrate was incubated with 12 μL reticulocyte lysate containing expressed wild-type or variant MSH2/MSH6 in the presence of buffers and cofactors. After 10 min incubation at 37°C, 75 μg HeLa extract was added and the reaction was incubated for an additional 25 min. Reactions were continued as described (5). Bars represent mean ± SEM. *$P < 0.05$ compared with WT. NS, Not significant. Partial, rather than complete, inhibition by the N671 variants was observed, as the substrate concentration exceeds the MSH2/MSH6 concentration.

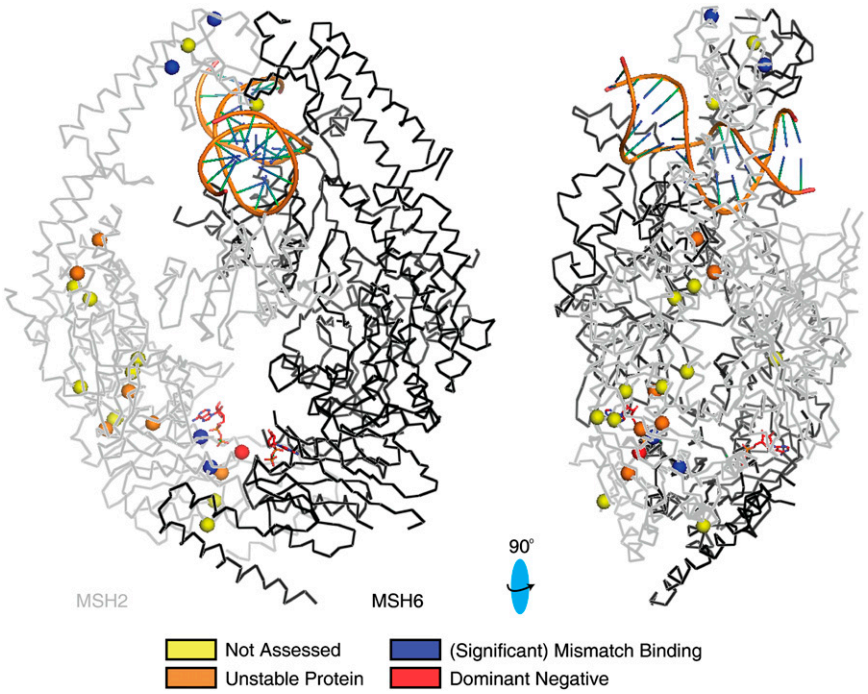

Fig. S3. Mapping of the residues mutated in our screen to the crystal structure of the human MSH2/MSH6 heterodimer. All residues are colored according to their in vitro phenotype. Gray, MSH2; black, MSH6. Mutated residues are shown as spheres.

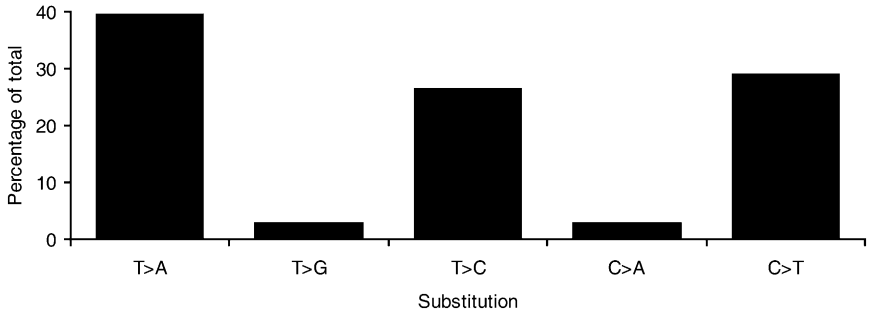

Fig. S4. Mutations induced by *N*-ethyl-*N*-nitrosourea at the *Msh2* allele. This spectrum illustrates the broad mutational capacity of *N*-ethyl-*N*-nitrosourea.

Table S1. Prototypic *Msh2* reverse diagnosis catalog

Mutation*	cDNA position	(codon change)	MAPP MMR†	Microsatellite Instability	In vivo protein level‡	Spontaneous mutator phenotype	Methylation tolerance	Repair in cell extracts	Complementation with wt MSH2/MSH6	Activity in CIMRA¶	Mismatch binding	ATP-induced Mismatch release	Corresponding VUS in LOVD
M148K	c.443	ATG > AAG	3.75	ND§	ND	ND	ND	ND	ND	ND	ND	ND	
I346N	c.1037	ATC > AAC	18.3	ND	ND	ND	ND	ND	ND	ND	ND	ND	
I356K	c.1067	ATA > AAA	14.66	ND	ND	ND	ND	ND	ND	ND	ND	ND	
I356R	c.1067	ATA > AGA	16.34	ND	ND	ND	ND	ND	ND	ND	ND	ND	
L407P	c.1220	CTG > CCG	18.56	+	−	+	+	−	+	−	ND	ND	L407L
L503P	c.1508	CTC > CCC	14.91	+	±	+	+	−	+	−	±	+	**L503P**
K546E	c.1636	AAG > GAG	23.7	ND	ND	ND	ND	ND	ND	ND	ND	ND	
N553K	c.1659	AAC > AAA	24.75	ND	ND	ND	ND	ND	ND	ND	ND	ND	
S557P	c.1669	TCC > CCC	9.71	+	±	+	+	−	+	−	±	ND	**T557P**
M592K	c.1775	ATG > AAG	8.21	+	−	+	+	−	+	−	ND	ND	M592V
L595P	c.1784	CTC > CCC	7.68	ND	ND	ND	ND	ND	ND	ND	ND	ND	
L599P	c.1796	CTG > CCG	17.42	ND	ND	ND	ND	ND	ND	ND	ND	ND	
G669D	c.2006	GGT > GAT	35.86	+	−	+	+	−	+	−	ND	ND	**G669D**/R
N671I‖	c.2012	AAT > ATT	22.05	+	+	+	+	−	−	−	+	−	
N671K‖	c.2013	AAT > AAA	25.31	+	+	+	+	−	−	−	+	−	**N671K**/Y
S676L	c.2027	TCA > TTA	28.64	+	+	+	+	−	+	−	+	+	S676P
G683R	c.2047	GGG > AGG	44	+	−	+	+	−	+	−	ND	ND	**G683R**/W
M688K	c.2063	ATG > AAG	32.5	+	−	+	+	−	+	−	ND	ND	M688R/I
V695E	c.2084	GTG > GAG	30.37	ND	ND	ND	ND	ND	ND	ND	ND	ND	
S699P	c.2095	TCG > CCG	5.97	ND	ND	ND	ND	ND	ND	ND	ND	ND	
A700E	c.2099	GCA > GAA	37.91	ND	ND	ND	ND	ND	ND	ND	ND	ND	
V702E	c.2105	GTG > GAG	33.26	+	−	+	+	−	+	−	ND	ND	V702G
E749G	c.2246	GAG > GGG	28.23	+	+	+	+	−	+	−	−	ND	
E749K	c.2245	GAG > AAG	19.98	+	+	+	+	−	+	−	±	+	**E749K**
G761R	c.2281	GGG > AGG	40.89	ND	ND	ND	ND	ND	ND	ND	ND	ND	
C822Y	c.2465	TGT > TAT	6.48	ND	ND	ND	ND	ND	ND	ND	ND	ND	

Boldface represents VUS that are identical in both the LOVD and the reverse diagnosis catalog.

*Amino acid position.

†In silico MAPP-MMR prediction of pathogenicity. Scores above 4.55 are predicted to be pathogenic, variant M148K is borderline pathogenic.

‡+, (near) wild type protein level; ±, reduced protein level; −, no protein.

¶CIMRA, complete In vitro MMR assay (Fig. 4*B*).

§ND, not determined (not in the validation panel).

‖Dominant-negative variant.